iScience

CellPress
OPEN ACCESS

Article

Mechanism that determines the economics of 100% renewable power systems

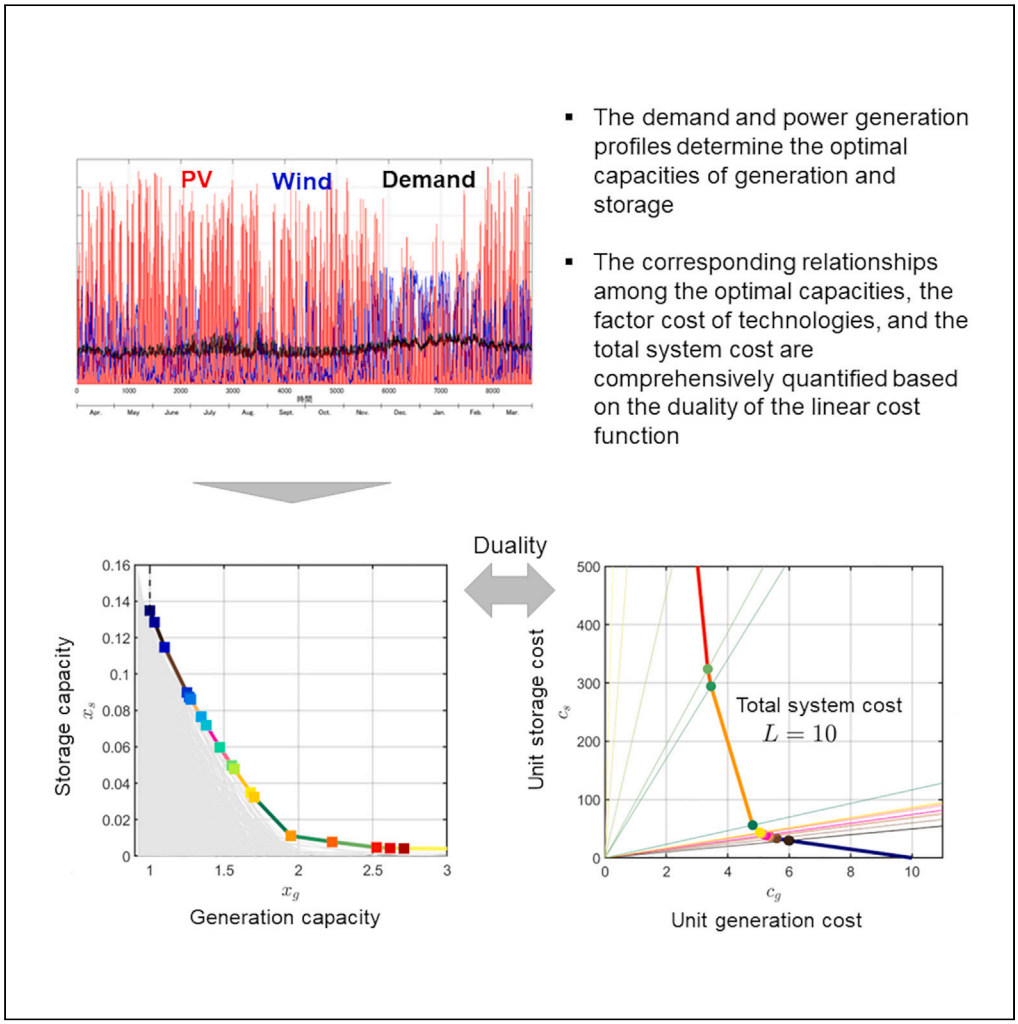

Takuya Hara

thara@mosk.tytlabs.co.jp

Highlights

Mathematical formulations of how profiles determine the optimal capacities

Correspondence between the optimal capacities and the costs of technologies

Mechanism of how hybrid renewable systems can reduce the total system cost

Hara, iScience *26*, 107872
October 20, 2023
https://doi.org/10.1016/j.isci.2023.107872

iScience

CellPress
OPEN ACCESS

Article

Mechanism that determines the economics of 100% renewable power systems

Takuya Hara[1,2,*]

SUMMARY

Many studies have evaluated the economic feasibility of 100% renewable power systems using the optimization approach, but the mechanisms determining the results remain unclear, making this issue still debatable. This study presents a mathematical formulation of the mechanism that only the demand and power generation profiles determine the optimal capacities of generation and storage and their trade-off relationship. Furthermore, this study demonstrates the comprehensive quantification of the corresponding relationships among the factor cost of technologies, their optimal capacities, and total system cost. Based on these findings, the study also shows that hybrid systems comprising multiple renewable energy sources and different types of storage, including long-duration energy storage, are critical to reducing the total system cost by using actual profile data for multiple years and regions in Japan. This suggests that large-scale deployment of current-level power-to-gas technologies, such as water electrolysis, can contribute to the economics of 100% renewable power systems.

INTRODUCTION

Amid calls for decarbonizing electricity as a means of mitigating climate change, researchers have evaluated the economics of highly decarbonized power systems, particularly in the form of 100% renewable energy power systems (100% REPS).[1] With a significant decline in the cost of variable renewable energy (VRE) technologies such as solar photovoltaics (PV) and wind turbines (WT)—for example, an 85% decline for PV and a 55% decline for WT over the last decades[2]—future deployment is expected to rapidly increase for both PV[3] and WT.[4] However, the economic feasibility of achieving 100% REPS remains debatable, particularly in the context of the US[5,6] and from a general perspective.[7,8]

The levelized cost of electricity (LCOE) is a common measure used to evaluate the cost competitiveness of power generation technologies. It is calculated by dividing the total life cycle cost by the total amount of power generated. As VRE requires energy storage to meet demand at all times, a hybrid system comprising VRE and energy storage is necessary to achieve 100% REPS. The LCOE of such a system (referred to as the levelized cost of hybrid system [LCOHS]) needs to consider not only the LCOE of VRE but also additional costs such as storage and overcapacity.[9,10]

The standard approach utilizes an optimization model, often formulated as linear programming (LP), to determine the optimal installed capacity and LCOHS. This approach has been applied in various contexts, including the US,[11] Japan,[12] and Chile.[13] The model treats the cost settings of VRE and storage, as well as the demand and generation profiles, as assumptions. The differences in evaluating LCOHS are attributed to variations in cost settings and profiles. However, the mechanisms by which these assumptions affect the results have remained unclear in the literature due to the challenges of using analytical models involving tens of thousands of variables.[14]

To address the knowledge gap in the economics of 100% REPS, this study examines the mechanisms that determine the optimal installed capacity and LCOHS using a simple yet essential model of 100% REPS, which includes demand, generation, and storage (refer to method details and supplemental information Figure S1). The study finds that the largest mismatch between demand and power generation profiles determines the optimal capacities of generation and storage, and it describes the relationship between cost settings, optimal capacities, and LCOHS. As the literature has overlooked the straightforward application of basic microeconomics, the findings of this study contribute to the understanding of the wide range of previous results[15,16] and provide a theoretical foundation for the economic benefits of mixing renewable sources (such as the complementarity of solar and wind)[17] and utilizing different types of storage.[11]

The contribution of this study is 2-fold. First, it presents a comprehensive method for identifying the combination of VRE and storage capacity for 100% REPS based solely on profile data (i.e., identifying the feasible region boundary of LP). Second, based on the identified feasible region boundary, it presents a method for establishing a comprehensive corresponding relationship between assumptions (i.e., cost settings) and results (i.e., optimal solutions) of LP-based 100% REPS.

To clarify the contribution of this study, the author provides a comparative review with relevant previous studies. The simple power system model used in this study can be interpreted in two ways: first, as a wide-area single-node grid model that disregards spatial variations of

[1]Toyota Central R&D Labs., Inc, Yokomichi 41-1, Nagakute, Aichi 480-1192, Japan
[2]Lead contact
*Correspondence: thara@mosk.tytlabs.co.jp
https://doi.org/10.1016/j.isci.2023.107872

generation/load profiles and transmission constraints/costs (or incorporates them into synthesized profiles and cost settings) under the copper plate assumption; second, as a stand-alone hybrid renewable energy system. Prior to the models and analyses of country-scale to global-scale 100% REPS, numerous studies have focused on the economics and optimal sizing of stand-alone systems.

In addition to LP, several methods have been proposed to optimize 100% REPS[18]: exploratory method, graphical construction method, and cumulative residual load method. The exploratory method, also known as the iterative simulation method, has been widely used. In this approach, power supply/charge/discharge processes at each time step are sequentially simulated under different combinations of VRE and storage capacities to find a set of capacities that enable 100% REPS or other criteria. Many previous studies have considered various hybrid systems, such as residential PV-battery system,[19] stand-alone PV-wind-battery system,[20,21] +pumped hydro storage system,[22] country-wide systems,[23] or various features such as the probability of failure[24] and specific load curves.[25,26] The combinations of VRE and storage capacities100% REPS obtained from these studies represent only a subset of the assumed combinations. By contrast, this study demonstrates that they can be expressed as a function of the generation/load profiles.

The graphical construction method, proposed in the 1980s, is essentially identical to this study in deriving comprehensive relationships between VRE and storage capacities for 100% REPS based solely on generation and load profiles.[27–29] The novelty of this study compared to the graphical construction method is that it presents a framework that can be analyzed at any time resolution, whereas previous studies typically had coarse time resolutions, such as monthly levels. The present study also contributes to a better understanding of the relationship between this method and LP.

The cumulative residual load method is used to determine the required amount of energy storage for a given VRE capacity and generation/load profile.[12,30,31] This study generalizes and extends the method, finding that the required energy storage for 100% REPS is equal to the largest difference between the partial sum of generation and demand profiles.

All the mentioned studies are related to the first contributions of this study, which involve identifying the feasible region boundary of LP. The graphical construction method is also relevant to the second contribution. It demonstrates how the determination of the cost-optimal solution is influenced by the relationship between the feasibility region boundary and the objective function. The novelty of this study lies in showing how the Legendre transform can be used to identify the correspondence between cost settings, optimal solutions, and system costs. Furthermore, it highlights that this relationship can exist irrespective of monetary units.

RESULTS

Production function of 100% renewable power system

Generalizing the findings of the cumulative residual load method, which demonstrates a strong relationship between cumulative residual load and the required energy capacity of storage, this study establishes the relationship between generation and storage capacity for a 100% REPS (x_g and x_s, respectively) using a piecewise linear function represented by Equation 1. This equation can be regarded as the production function (or isoquant) for a 100% REPS, as it represents the combination of production factors (in this case, generation and storage) required.

$$x_s = \max\left(-x_g \boldsymbol{G} + \boldsymbol{D}\right) \quad \text{(Equation 1)}$$

$\boldsymbol{G}, \boldsymbol{D}$ is a matrix where the (i, j) component represents the partial sum of the generation and demand profiles during the period i and j (refer to method details). Equation 1 demonstrates that the storage requirement is determined by the magnitude of the difference between the total demand and total generation during the bottleneck period, which refers to the period with the largest difference (refer to method details and Figure S2). The bottleneck can be identified by searching for the boundary of the convex hull formed by pairs of the coefficient G_{ij} and intercepts D_{ij} on the (G, D) plane, utilizing the duality of linear function (refer to method details and Figure S3). While previous studies have suggested a connection between storage requirement and the occurrence of continuous supply shortages (referred to as "dark doldrums" or "Dunkelflaute"),[12,13] this study provides a clear formulation for this relationship.

Figure 1 illustrates the calculation results using the demand and PV generation profiles for the Tohoku region in Japan in 2018 (refer to supplemental information). Through profile normalization, x_g and x_s (as well as G_{ij} and D_{ij}) represent the total generation and storage requirements (partial sum of unit generation and demand) as a proportion of the total demand, respectively. In Figure 1A, the points and the boundary of the convex hull are presented, while Figure 1B depicts Equation 1 based on the results from Figure 1A. When the total generation matches the total demand (i.e., $x_g = 1$), the storage requirement amounts to approximately 50 days' worth of demand (i.e., $x_s \sim 0.135$). As the generation increases, the storage requirement decreases rapidly to 3–4 days' worth of demand ($x_s \sim 0.01$ when $x_g > 2$), and so does the bottleneck period.

Cost function of 100% renewable power system

The LCOHS of a 100% REPS, L, can be represented by a linear equation (Equation 2) involving the LCOE and the capacity of generation and storage (c_g, c_s, x_g, x_s, respectively), similar to the objective function of the LP model (refer to method details and supplemental information):

$$L = c_g x_g + c_s x_s \quad \text{(Equation 2)}$$

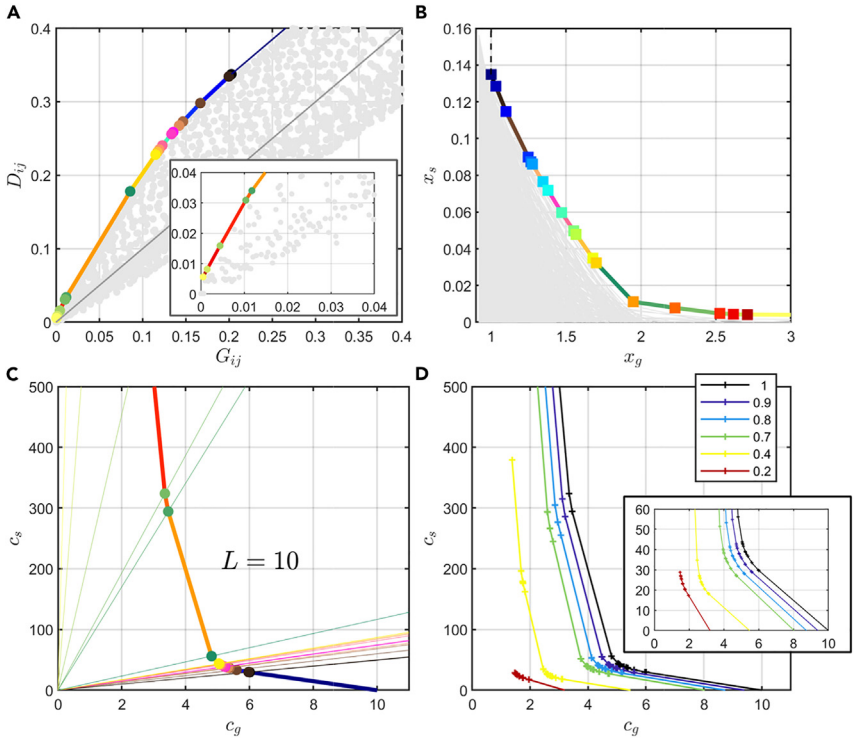

Figure 1. Production function (generation + storage capacity) and cost function of 100% REPS determined from demand and generation profiles

(A) Combination of the partial sum of unit generation and demand: The colored circle points and lines represent points and lines on the boundary of the convex hull of the point set. The gray points depict points inside the boundary—the inset is an enlarged view.

(B) Combination of generation and storage capacity, derived from the dual transform of (A) The colored lines represent piecewise linear functions of generation and storage capacity for 100% REPS. The lines in (B) correspond to the circle points in (A) of the same color. The colored square points denote extreme points of the feasible region of the equivalent LP model. These square points have corresponding points in (B) and lines in (A) of the same color.

(C) Cost function representing the combination of LCOE of generation and storage, where LCOHS is an arbitrary value (e.g., $L = 10$), derived from Legendre transform of (B). The corresponding straight lines originating from the origin in (C), circle points in (A), and lines in (B) are in the same color. The circle points in (C) represent the (c_g, c_s) combination at $L = 10$. The lines between the circle points in (C), which represent the optimal capacity under LCOE, and the square points in (B), as well as the lines in (A), are shown in the same color.

(D) Cost functions obtained with different charge/discharge efficiencies of storage—the inset is an enlarged view.

The minimum cost required to achieve a specific level of production, in this case, 100% REPS, expressed as a function of factor prices (in this case, LCOE), is referred to as a cost function. Once the cost function for a 100% REPS is determined, the relationship between LCOE and LCOHS can be comprehensively understood. Following a fundamental theorem of microeconomics (specifically, a Legendre transform), the cost function can be derived from the isoquant (refer to ref. 32 and supplemental information Figure S4). The isoquant also represents the connection between the partial sums of profiles in the bottleneck periods and the optimal capacity. Consequently, it implies that the relationship between the partial sum of profiles, the LCOE, and the LCOHS can be quantified. This study reveals that the LCOEs required to achieve any given LCOHS are solely determined by the profiles and can be expressed in Equation 3, where (G^*, D^*) are the combination of the partial sum of generation and demand during the bottleneck period.

$$(c_g, c_s) = \left(\frac{G^*}{D^*}L, \frac{1}{D^*}L\right) \quad \text{(Equation 3)}$$

Figure 1C illustrates Equation 3 and demonstrates the correspondence between these factors represented by points and lines of the same color in Figures 1A and 1B (refer to supplemental information Figure S4 as well). It is important to note that Equations 2 and 3 are unit-independent due to the use of normalized variables. This means that the quantitative relationship remains the same regardless of the chosen unit, such as JPY/kWh, USD/GJ, and so on. While Figure 1C only displays one line ($L = 10$) as an example, it provides sufficient information, as Equations 2 and 3 exhibit linear homogeneity. In other words, once one line $L_0(c_g, c_s)$ is obtained, any other combination of LCOEs at $L = aL_0$ can be obtained proportionally as (ac_g, ac_s) (refer to supplemental information Figure S5).

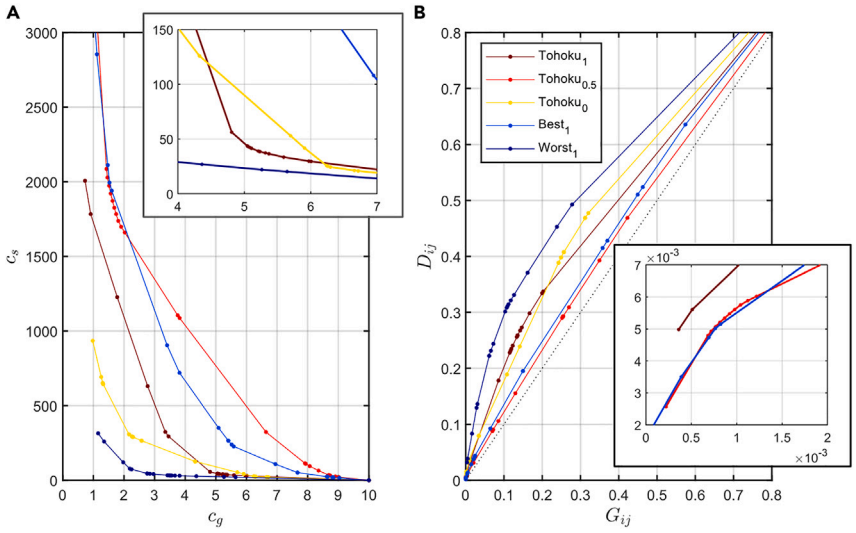

Figure 2. Cost functions obtained with different PV ratios and profiles

(A) Various cost functions obtained with different preconditions, assuming a charge/discharge efficiency of 1. Tohoku$_1$ is the same function as Figure 1C; Tohoku$_{0.5}$ and Tohoku$_0$ are cost functions with PV ratio = 0.5 and 0 (the rest from WT), respectively; Best$_1$ and Worst$_1$ represent the best and worst economic feasibility amounts for the profiles of different regions/years with PV ratios of 1—the inset is an enlarged view.

(B) Combination of partial sum of unit generation and demand corresponding to the profiles in (A). The diagonal line ($D = G$) is in black—the inset is an enlarged view. The profiles in (A) show that for the same c_g, the one with a higher c_s (higher cost tolerance for storage, or better economic feasibility) to achieve the same LCOHS ($L = 10$) is represented in (B) as the one with the same G_{ij} and lower D_{ij}. The economics of 100% REPS of different profiles can be explained by the relationship between the size of the partial sums of profiles.

Figures 1A–1C depict the results when there is no charge/discharge loss. Figure 1D illustrates the cost functions ($L = 10$) obtained with different storage charge/discharge efficiencies. In order to emphasize the practical implications, the study employed JPY/kWh (roughly equivalent to cent/kWh) and $L = 10$ as the criteria for economic feasibility (refer to method details). The generation and storage cost conditions for $L = 10$ are as follows: for high-efficiency storage (cycle efficiency 0.7–1), when the generation cost is relatively high (c_g = 5–10 JPY/kWh), the storage cost needs to be very low ($c_s = \sim 30$ JPY/kWh). When the generation cost can be relatively low (c_g = 2–4 JPY/kWh), the storage costs can be somewhat high (c_s = 100–500 JPY/kWh), but the allowable storage cost is still one digit lower than the current battery cost (refer to ref. 11 and supplemental information). For low-efficiency storage (cycle efficiency 0.2–0.4), high generation costs render any allowable storage cost ineffective. However, at low generation costs, an economically feasible 100% REPS can still be achieved with sufficiently low storage costs.

Mechanism of economic feasibility dependent on profile

How do the economics differ among the different profiles, and to what extent does the formulation of this study explain these differences? Figure 2A illustrates the cost functions derived from the results of the best and worst (PV-only case) among the 30 profiles utilized in the study (all results can be found in supplemental information Figure S7). The figure also depicts the outcomes for the same profile (Tohoku, as shown in Figure 1C) with varying PV ratios.

Figure 2A illustrates that different cost conditions are necessary for different profiles in order to achieve the same LCOHS. The relationship of relative advantage between the profiles ($c_g - c_s$ curve) is complex. However, it can be explained by the variation in the combination of the partial sum of unit generation and demand ($G - D$ curve), as shown in Figure 2B. The observed trend is that the closer the $G - D$ curve is to the diagonal, the farther the $c_g - c_s$ curve is from the origin. This indicates that such profiles are more economical, as they can achieve the same LCOHS at a higher LCOE. The differences in the value of G at the same D across different profiles account for the disparities in the cost functions of these profiles. In other words, Equation 3 enables economic comparisons among different profiles as well (refer to supplemental information Figure S5).

Figure 2A demonstrates that the profile comprising an equal combination of PV and WT (Tohoku$_{0.5}$) is more economical than the profile with only one source. This can be understood by considering the formula for determining the required storage capacity (Equation 1), which also serves as the energy balance formula for the bottleneck period. In other words, during the bottleneck period determined by the generation profile of either PV or WT alone, if the partial sum of the WT (PT) unit generation profile is larger, the value of G increases when a small amount of WT (PV) is introduced. Consequently, this results in a reduction in storage requirements and improved economics. This mechanism explains why synthesizing PV and WT generally leads to better economics compared to using only one source, with a few exceptional cases (refer to supplemental information Figures S10 and S11). Advantages of multi-sources and multi-types of storage

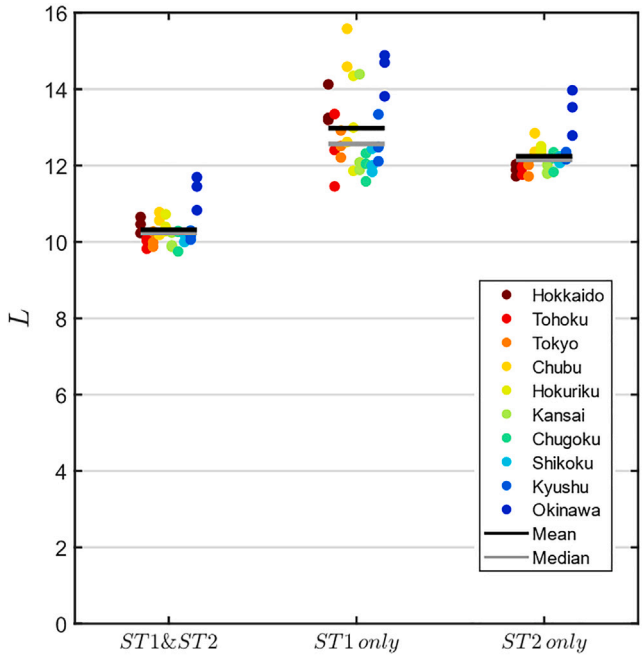

Figure 3. Cost comparison for systems comprising different storage types

LCOHSs (*L*) from the three-year profile are depicted using different colors for each of the 10 regions. The cost settings of technologies (coefficients of the objective function in the LP model) are determined through preliminary calculations, ensuring that the LCOHS of the Tohoku profiles is set at 10 JPY/kWh (refer to method details). It is evident that the LCOHS of the ST1&ST2 system is consistently more cost-efficient compared to those of the ST1 or ST2 systems.

Figure 1D illustrates that storage with higher efficiency allows for a higher allowable cost to achieve a specific LCOHS, while storage with lower efficiency becomes feasible if the cost is sufficiently low. This study discovered that if two types of storage are available, it is always possible to reduce LCOHS and the variance attributed to profile differences.

The first storage type (ST1) is assumed to be a battery with a cycle efficiency of 0.8, and the second storage type (ST2) is assumed to be a power-to-gas-to-power system, serving as long-duration energy storage with an efficiency of 0.4.[11,12] The cost of storage and required power capacity are also taken into account. For ST2, this study considers water electrolysis for the power-to-gas process and a hydrogen-fired combined cycle gas turbine for the gas-to-power process. The LCOHS of three systems is calculated using the LP model: ST1&ST2, ST1 only, and ST2 only (refer to supplemental information). The cost settings for each technology are determined through preliminary calculations (refer to supplemental information Figure S9). Compared to the cost setting for generation and ST1, the cost setting for ST2 is conservative, aiming to reflect current levels (refer to supplemental information Tables S1 and S2).

Figure 3 displays the LCOHS for the 30 profiles (10 regions in Japan [see Figure S8], three years, PV : WT = 1 : 1) for the three systems, clearly demonstrating that the ST1&ST2 system is economically superior to the ST1 or ST2-only systems for all profiles. This mechanism can also be understood by examining the energy balance during the bottleneck period (refer to supplemental information). Intuitively, the advantage of introducing ST1 into an ST2-only system can be explained by the mechanism through which ST1 increases the surplus power available during the bottleneck period due to its higher efficiency. The introduction of ST1 also reduces the duration of the bottleneck period by improving the efficiency of surplus power utilization. The merit of introducing ST2 into an ST1-only system lies in the lower cost of stored energy for ST2, which outweighs the disadvantage of its lower efficiency.

DISCUSSION

A 100% REPS comprising PV and WT with ST1&ST2 can be economically viable even at the current achievable level of storage cost. This finding aligns with that of previous studies,[11] and the present study provides the fundamental mechanism underlying these results. The crucial factor determining feasibility is the amount of VRE supply required to achieve the desired LCOE, emphasizing the need for accurate estimates of physical, economic, and socio-political potential.

A more robust 100% REPS objective would result in overcapacity in most typical year profiles, as supply shortages must be entirely avoided. By using more conservatively updated *G* and *D* based not only on historical profiles but also on risk assumptions, the methodology simplifies estimating additional capacity and costs.

A robust 100% REPS would entail the widespread deployment of ST2, involving substantial cumulative production of water electrolyzers and a surplus of renewable hydrogen, which serves as the energy carrier for ST2. Intersectoral hydrogen energy systems can contribute to

100% REPS by reducing backup costs through shared facilities.[16] As renewable technologies and hydrogen production technologies scale up, subsequent cost reductions would make large-scale deployment of cost-effective renewable hydrogen possible. This broad vision leads from a renewable energy-driven power sector toward decarbonized energy systems.

While the normalization of profile data/variables enables unit-independent economic evaluation, it is important to note that some numerical conversions may be necessary to utilize this information for real-world decisions, such as R&D target setting and investment/policy design (refer to supplemental information).

This study demonstrates that the bottleneck, determined by the largest mismatch between demand and power generation profiles, decides the optimal capacities of generation and storage. The bottleneck can be identified by searching the convex hull of the set of partial sums of demand and generation profiles. Blanford et al.[33] show that "extreme hours" (similar to the concept of bottleneck in this study), identified through the convex hull of generation and demand profiles, are useful for appropriately designing time-slices in power system modeling. While their model does not include energy storage, their results suggest that the concept of bottleneck can be extended to renewable power systems at any level, not limited to 100% REPS, and may help address the significant issue in the literature of designing power system models to obtain accurate results with lower temporal resolution.[34]

For the sake of simplicity, the model does not account for inevitable constraints in 100% REPS, such as transmission capacity, flexibility, and inertia. The first two can be addressed by the ST1&ST2 system, and the cost of transmission to connect VRE to demand can be practically considered by including it in the LCOE of generation.[8]

Additionally, the model does not factor in self-discharge, leading to an underestimation of the required storage capacity and introducing an underestimation bias in LCOHS. To compensate for this bias, additional estimates are necessary. As demonstrated in this study, the storage capacity for 100% REPS is determined by the difference between the partial sum of generation and demand profiles during the bottleneck period. This means that the amount of power lost due to self-discharge can be relatively easily estimated, as the length of the bottleneck period and the length of the charging period leading up to full charge just before the bottleneck period can be identified. Consequently, it becomes possible to estimate the results when self-discharge is taken into account, based on the results from a model that neglects self-discharge. It is important to note that other important factors, such as the cost of transmission for remote VRE sources, aging of VRE generation efficiency (capacity factor degradation), aging of storage (storage energy capacity degradation), and SOC range, are not considered in this model. These potential biases arising from the omission of these factors can be compensated for by considering the model parameters as values that incorporate these factors in advance.

The simplicity of the model facilitates a comprehensive understanding of the relationship between assumptions (LCOE) and results (optimal capacity and LCOHS) for 100% REPS. This simplicity enables the identification of the mechanism that determines optimal solutions and further reveals that the mechanism also applies to more complex systems. This insight highlights the importance of expanding long-term, low-cost storage (such as hydrogen) to achieve a robust 100% REPS.

The appropriately abstracted model allows for the application of the same framework across various scales, from a residence to a national grid. The simple model elucidates the mechanism,[35] while the realistic complex model enables analyses that assist in designing and implementing feasible decarbonized power systems, taking into account the local context.

Limitations of the study

This study relies on limited Japanese profile data; thus, further examination of results across various profiles (including historical profiles of different regions or hypothetical ones for future planning) is needed before making more general claims.

The model employed in this study is a simplified one, designed to understand the underlying mechanism. As discussed in the previous section, when evaluating costs based on the results, it is crucial to apply appropriate corrections and interpretations. This is necessary because there may be biases introduced by not accounting for critical factors associated with the simplification process.

STAR★METHODS

Detailed methods are provided in the online version of this paper and include the following:

- KEY RESOURCES TABLE
- RESOURCE AVAILABILITY
  - Lead contact
  - Materials availability
  - Data and code availability
- METHOD DETAILS
  - Derivation of production function of 100% renewable power systems
- THE CORRESPONDING LINEAR PROGRAMMING MODEL
- BOTTLENECK PERIOD
  - Duality of linear function
  - Profile data
  - Criterion of economic feasibility for Japan's context

SUPPLEMENTAL INFORMATION

Supplemental information can be found online at https://doi.org/10.1016/j.isci.2023.107872.

ACKNOWLEDGMENTS

The author thanks the members of the energy systems design program at Toyota Central R&D Labs. for their helpful comments.

AUTHOR CONTRIBUTIONS

T.H. conceived and designed the study, developed the model, implemented the analysis, and wrote the manuscript.

DECLARATION OF INTERESTS

The author declares no competing interests.

Received: February 15, 2023
Revised: July 26, 2023
Accepted: September 6, 2023
Published: September 9, 2023

REFERENCES

1. Khalili, S., and Breyer, C. (2022). Review on 100% Renewable Energy System Analyses - A Bibliometric Perspective. IEEE Access *10*, 125792–125834. https://doi.org/10.1109/ACCESS.2022.3221155.
2. Shukla, P.R., Skea, J., Reisinger, A., Slade, R., Fradera, R., Pathak, M., Al, A., Malek, K., Renée Van Diemen, B., Hasija, A., et al. (2022). Climate Change 2022 Mitigation of Climate Change Working Group III Contribution to the Sixth Assessment Report of the Intergovernmental Panel on Climate Change Summary for Policymakers (IPCC).
3. Haegel, N.M., Atwater, H., Barnes, T., Breyer, C., Burrell, A., Chiang, Y.M., De Wolf, S., Dimmler, B., Feldman, D., Glunz, S., et al. (2019). Terawatt-scale photovoltaics: Transform global energy Improving costs and scale reflect looming opportunities. Science *364*, 836–838. https://doi.org/10.1126/SCIENCE.AAW1845.
4. Wiser, R., Jenni, K., Seel, J., Baker, E., Hand, M., Lantz, E., and Smith, A. (2016). Expert elicitation survey on future wind energy costs. Nat. Energy *1*, 16135. https://doi.org/10.1038/NENERGY.2016.135.
5. Jacobson, M.Z., Delucchi, M.A., Cameron, M.A., and Frew, B.A. (2015). Low-cost solution to the grid reliability problem with 100% penetration of intermittent wind, water, and solar for all purposes. Proc. Natl. Acad. Sci. USA. *112*, 15060–15065. https://doi.org/10.1073/pnas.1510028112.
6. Clack, C.T.M., Qvist, S.A., Apt, J., Bazilian, M., Brandt, A.R., Caldeira, K., Davis, S.J., Diakov, V., Handschy, M.A., Hines, P.D.H., et al. (2017). Evaluation of a proposal for reliable low-cost grid power with 100% wind, water, and solar. Proc. Natl. Acad. Sci. USA. *114*, 6722–6727. https://doi.org/10.1073/pnas.1610381114.
7. Heard, B.P., Brook, B.W., Wigley, T.M.L., and Bradshaw, C.J.A. (2017). Burden of proof: A comprehensive review of the feasibility of 100% renewable-electricity systems. Renew. Sustain. Energy Rev. *76*, 1122–1133. https://doi.org/10.1016/j.rser.2017.03.114.
8. Brown, T.W., Bischof-Niemz, T., Blok, K., Breyer, C., Lund, H., and Mathiesen, B.V. (2018). Response to 'Burden of proof: A comprehensive review of the feasibility of 100% renewable-electricity systems. Renew. Sustain. Energy Rev. *92*, 834–847. https://doi.org/10.1016/j.rser.2018.04.113.
9. Ueckerdt, F., Hirth, L., Luderer, G., and Edenhofer, O. (2013). System LCOE: What are the costs of variable renewables? Energy *63*, 61–75. https://doi.org/10.1016/J.ENERGY.2013.10.072.
10. Lai, C.S., and McCulloch, M.D. (2017). Levelized cost of electricity for solar photovoltaic and electrical energy storage. Appl. Energy *190*, 191–203. https://doi.org/10.1016/j.apenergy.2016.12.153.
11. Dowling, J.A., Rinaldi, K.Z., Ruggles, T.H., Davis, S.J., Yuan, M., Tong, F., Lewis, N.S., and Caldeira, K. (2020). Role of Long-Duration Energy Storage in Variable Renewable Electricity Systems. Joule *4*, 1907–1928. https://doi.org/10.1016/j.joule.2020.07.007.
12. Matsuo, Y., Endo, S., Nagatomi, Y., Shibata, Y., Komiyama, R., and Fujii, Y. (2020). Investigating the economics of the power sector under high penetration of variable renewable energies. Appl. Energy *267*, 113956. https://doi.org/10.1016/j.apenergy.2019.113956.
13. Haas, J., Cebulla, F., Nowak, W., Rahmann, C., and Palma-Behnke, R. (2018). A multi-service approach for planning the optimal mix of energy storage technologies in a fully-renewable power supply. Energy Convers. Manag. *178*, 355–368. https://doi.org/10.1016/j.enconman.2018.09.087.
14. Denholm, P., Arent, D.J., Baldwin, S.F., Bilello, D.E., Brinkman, G.L., Cochran, J.M., Cole, W.J., Frew, B., Gevorgian, V., Heeter, J., et al. (2021). The challenges of achieving a 100% renewable electricity system in the United States. Joule *5*, 1331–1352. https://doi.org/10.1016/j.joule.2021.03.028.
15. Pfenninger, S. (2017). Dealing with multiple decades of hourly wind and PV time series in energy models: A comparison of methods to reduce time resolution and the planning implications of inter-annual variability. Appl. Energy *197*, 1–13. https://doi.org/10.1016/j.apenergy.2017.03.051.
16. Schill, W.P. (2020). Electricity Storage and the Renewable Energy Transition. Joule *4*, 2059–2064. https://doi.org/10.1016/J.JOULE.2020.07.022/.
17. Cebulla, F., Haas, J., Eichman, J., Nowak, W., and Mancarella, P. (2018). How much electrical energy storage do we need? A synthesis for the U.S., Europe, and Germany. J. Clean. Prod. *181*, 449–459. https://doi.org/10.1016/j.jclepro.2018.01.144.
18. Khan, F.A., Pal, N., and Saeed, S. (2018). Review of solar photovoltaic and wind hybrid energy systems for sizing strategies optimization techniques and cost analysis methodologies. Renew. Sustain. Energy Rev. *92*, 937–947. https://doi.org/10.1016/j.rser.2018.04.107.
19. Weniger, J., Tjaden, T., and Quaschning, V. (2014). Sizing of Residential PV Battery Systems. Energy Proc. *46*, 78–87. https://doi.org/10.1016/J.EGYPRO.2014.01.160.
20. Yang, H., Lu, L., and Zhou, W. (2007). A novel optimization sizing model for hybrid solar-wind power generation system. Sol. Energy *81*, 76–84. https://doi.org/10.1016/j.solener.2006.06.010.
21. Diaf, S., Diaf, D., Belhamel, M., Haddadi, M., and Louche, A. (2007). A methodology for optimal sizing of autonomous hybrid PV/wind system. Energy Pol. *35*, 5708–5718. https://doi.org/10.1016/j.enpol.2007.06.020.
22. Canales, F.A., Jurasz, J.K., Guezgouz, M., and Beluco, A. (2021). Cost-reliability analysis of hybrid pumped-battery storage for solar and wind energy integration in an island community. Sustain. Energy Technol. Assessments *44*, 101062. https://doi.org/10.1016/j.seta.2021.101062.
23. Budischak, C., Sewell, D., Thomson, H., MacH, L., Veron, D.E., and Kempton, W. (2013). Cost-minimized combinations of wind power, solar power and electrochemical storage, powering the grid up to 99.9% of the time. J. Power Sources *225*, 60–74. https://doi.org/10.1016/j.jpowsour.2012.09.054.
24. DaneshvarDehnavi, S., Negri, C.A., Giesselmann, M.G., Bayne, S.B., and Wollenberg, B. (2021). Can 100% renewable power system be successfully built? Renew. Energy *177*, 715–722. https://doi.org/10.1016/j.renene.2021.06.002.
25. Braff, W.A., Mueller, J.M., and Trancik, J.E. (2016). Value of storage technologies for wind

and solar energy. Nat. Clim. Change *6*, 964–969. https://doi.org/10.1038/nclimate3045.

26. Gupta, R., Soini, M.C., Patel, M.K., and Parra, D. (2020). Levelized cost of solar photovoltaics and wind supported by storage technologies to supply firm electricity. J. Energy Storage *27*, 101027. https://doi.org/10.1016/j.est.2019.101027.
27. Gordon, J.M. (1987). Optimal sizing of stand-alone photovoltaic solar power systems. Sol. Cell. *20*, 295–313. https://doi.org/10.1016/0379-6787(87)90005-6.
28. Markvart, T. (1996). Sizing of hybrid photovoltaic-wind energy systems. Sol. Energy *57*, 277–281. https://doi.org/10.1016/S0038-092X(96)00106-5.
29. Borowy, B.S., and Salameh, Z.M. (1996). Methodology for Optimally Sizing the Combination of a Battery Bank and PV Array in a Wind/PV Hybrid System. IEEE Trans. On energy Conversion *11*, 367–375. https://doi.org/10.1109/60.507648.
30. Arai, T., and Noro, Y. (2017). Examination of possibility of supply by renewable energy and storage battery. Proc. Annu. Meet. IEEJ, 102–103. (in Japanese).
31. Aratame, K. (2018). Stable supplying costs of photovoltaic and wind generating electricity. IEEJ Trans. PE. *138*, 451–459. (in Japanese).
32. Hara, T. (2019). Simplified analysis of the relationships between the prices and optimal capacities of PV systems and batteries. Int. Associ. Ene. Econ. Annual Conference *42*, 16164.
33. Blanford, G.J., Merrick, J.H., Bistline, J.E., and Young, D.T. (2018). Simulating Annual Variation in Load, Wind, and Solar by Representative Hour Selection. Energy J *39*, 189–212. https://doi.org/10.5547/01956574.39.3.gbla.
34. Teichgraeber, H., and Brandt, A.R. (2022). Time-series aggregation for the optimization of energy systems: Goals, challenges, approaches, and opportunities. Renew. Sustain. Energy Rev. *157*, 111984. https://doi.org/10.1016/j.rser.2021.111984.
35. Levi, P.J., Kurland, S.D., Carbajales-Dale, M., Weyant, J.P., Brandt, A.R., and Benson, S.M. (2019). Macro-Energy Systems: Toward a New Discipline. Joule *3*, 2282–2286. https://doi.org/10.1016/J.JOULE.2019.07.017.
36. (2022). OCCTO. https://www.occto.or.jp/en.
37. (2021). METI. Report on power generation cost verification. (in Japanese). https://www.enecho.meti.go.jp/committee/council/basic_policy_subcommittee/mitoshi/cost_wg/pdf/cost_wg_20210908_01.pdf.

STAR★METHODS

KEY RESOURCES TABLE

REAGENT or RESOURCE	SOURCE	IDENTIFIER
Deposited data	Zenodo	https://doi.org/10.5281/zenodo.8283187
Demand and generation profile (solar and wind), 10 regions in Japan, 3 years (fiscal year 2016–2018), and hourly time series data	Organization for Cross-regional Coordination of Transmission Operators, JAPAN (OCCTO)	https://www.occto.or.jp/en
Software	MATLAB R2021b Optimization Toolbox	https://www.mathworks.com/

RESOURCE AVAILABILITY

Lead contact

Further information and requests for resources and reagents should be directed to and will be fulfilled by the lead contact, Takuya Hara (thara@mosk.tytlabs.co.jp).

Materials availability

This study did not generate any new unique reagents. All datasets and codes used in this study will be available from Zenodo (https://doi.org/10.5281/zenodo.8283187).

Data and code availability

- All datasets have been deposited at Zenodo and is publicly available as of the date of publication. DOIs are listed in the key resources table.
- All original code has been deposited at Zenodo and is publicly available as of the date of publication. DOIs are listed in the key resources table.
- Any additional information required to reanalyze the data reported in this paper is available from the lead contact upon request.

METHOD DETAILS

Derivation of production function of 100% renewable power systems

First, consider the difference of generation and demand in t, termed residual load, and r_t, defined as follows,

$$r_t = x_g g_t - d_t \quad \text{(Equation 4)}$$

where d_t is demand, g_t is generated electricity per unit capacity, and x_g is VRE capacity.

Positive (negative) r_t means a surplus (deficit) of generation to meet demand. Demand and generation profiles are normalized to yield an equal total. The profile is assumed to have periodic boundary conditions.

100% REPS is achieved as follows: for every negative residual load $r_t < 0$, the surplus $r_{t'} > 0$ generated in earlier time $t' < t$ must be charged in storage and discharged to fill the deficit.

Cumulative residual load Q_{ij} is the sum of residual load in period $t = i \sim j$.

$$Q_{ij} = \sum_{t=i}^{j} r_t \quad \text{(Equation 5)}$$

Assume $Q_{ij} < 0$: supply from storage is necessary to meet the demand in period $t = i \sim j$. The required condition of storage to meet the demand of the period is that the charged electricity is $-Q_{ij}$ at the end of $t = i - 1$. Thus, the required capacity of storage is $x_s \geq -Q_{ij}$.

In the period other than $t = i \sim j$, that is, $t = j+1 \sim i-1$, the generation surplus is always larger than $-Q_{ij}$ because of the following equation expansion (T = total number of time steps).

$$x_s \geq -Q_{ij} \sum_{t=j+1}^{i-1} r_t = \sum_{t=1}^{T} r_t - \sum_{t=i}^{j} r_t = \sum_{t=1}^{T} r_t - Q_{ij} \geq -Q_{ij} \quad \text{(Equation 6)}$$

Therefore, in the period $t = i \sim j$, the required capacity of storage is $x_s = \max(-Q_{ij}, 0)$ when considering both cases of $Q_{ij} < 0$ and $Q_{ij} \geq 0$.

For a given demand and generation profile, the amount of storage required for 100% REPS can be determined by finding the maximum of all combinations of the periods as

$$x_s = \max(-\boldsymbol{Q}) \quad \text{(Equation 7)}$$

where $\boldsymbol{Q}$ is a matrix whose (i, j) component is jQ_i.

Equations (Equations 4, 5 and 7) yield

$$x_s = \max\left(-x_g\boldsymbol{G} + \boldsymbol{D}\right) \quad \text{(Equation 8)}$$

where, similarly, $\boldsymbol{G}$, $\boldsymbol{D}$ is a matrix whose (i, j) component, G_{ij} and D_{ij}, is the partial sum of the generation and demand profile.

Arai and Noro,[30] Aratame,[31] and Matsuo et al.[12] independently discovered a strong relationship between cumulative residual load and the required energy capacity of storage for 100% REPS. The difference between the maximum and minimum cumulative residual load is equivalent to the required energy capacity of storage under the assumption of zero charge/discharge loss.[30,31] Matsuo et al.[12] also considered the effects of charge/discharge loss and self-discharging. To the best of the author's knowledge, no other studies have identified this relationship. Therefore, this study builds upon the recognition of the significance of cumulative residual load for 100% REPS highlighted in these three studies. It expands and generalizes the formulation to identify the mechanism that determines the economics of 100% REPS. Consequently, this study reveals that Equation (Equation 8) corresponds to the boundary of the feasible region in the simplest LP model, as discussed in the following section.

THE CORRESPONDING LINEAR PROGRAMMING MODEL

As an initial step, let us consider the simplest LP model to determine the optimal configuration of the system, which includes the following elements: generation, demand, and storage, with each element of a single type. For storage, let us only consider energy capacity without considering charge/discharge loss. The LP model can be formulated as follows.

$$\min_{x_g, x_s, x_{it}} L = c_g x_g + c_s x_s + 0 \sum_{t=1}^{T} (x_{1t} + x_{2t} + x_{3t} + s_t) \quad \text{(Equation 9)}$$

$$\text{subject to } x_{1t} + x_{2t} \leq x_g g_t \quad \text{(Equation 10)}$$

$$x_{1t} + x_{3t} = d_t \quad \text{(Equation 11)}$$

$$x_{2t} - x_{3t} + s_{t-1} = s_t \quad \text{(Equation 12)}$$

$$s_t \leq x_s \quad \text{(Equation 13)}$$

Here, the objective function is the LCOHS L, and the coefficients of the objective function, c_g and c_s, are the unit costs (LCOE) of generation and storage, respectively. For a simple representation of LCOE, see supplemental information and Figure S6.

In this LP model, the energy flow at each time step t is explicitly considered a variable. Let x_{1t} be the flow of energy generated and directly supplied to demand, x_{2t} be the energy charged from generation to storage, x_{3t} be the flow supplied (discharged) from storage to demand, and s_t be the amount of charge in storage (after charging and discharging at t).

In the objective function, the coefficients of the energy flows are zero. The imposed constraints guarantee energy balance at the generation facility, demand, and storage, respectively. All variables are non-negative. The number of variables is $2+4T$, and the number of constraint equations is $4T$.

The schematic diagram of the system is shown in Figure S1A.

The constraints Equations (Equations 10–12) yield Equation (Equation 14).

$$x_g g_t - d_t \geq s_t - s_{t-1} \quad \text{(Equation 14)}$$

Consider the sum of Eq for period $t = i \sim j$. The minimum difference between the amount of charge at $t = i - 1$ and $t = j$ $(\min(s_j - s_{i-1}))$ is equal to the difference between the minimum (0) and maximum (x_s) values of the amount of charge, or $-x_s$. Thus,

$$x_g \sum_{t=i}^{j} g_t - \sum_{t=i}^{j} d_t \geq s_j - s_{i-1} \geq \min_{i,j}(s_j - s_{i-1}) = \min_j(s_j) - \max_i(s_{i-1}) = -x_s \quad \text{(Equation 15)}$$

Further transforming Equation (Equation 15) yields

$$x_s \geq -x_g \sum_{t=i}^{j} g_t + \sum_{t=i}^{j} d_t \quad \text{(Equation 16)}$$

From the aforementioned equations, the LP model ($2+4T$ variables and $4T$ constraints [shown in Equations (Equations 10–13)]) can be transformed into an equivalent LP model of 2 variables and T^2 constraints (shown in Equation (Equation 16)) with the following objective function.

$$\min_{x_g, x_s} L = c_g x_g + c_s x_s \quad \text{(Equation 17)}$$

The boundary of the feasible region of the LP model expressed by Equation (Equation 16) becomes the piecewise linear function shown as Equation 1 in the main text (and Equation 8).

BOTTLENECK PERIOD

The piecewise linear function representing the combination of generation and storage capacity for 100% REPS indicates that the required storage capacity is determined by the period in which the difference between the partial sum of demand and generation is the largest, within a certain range of generation capacity, as shown in Equation (Equation 18).

$$x_s = \sum_{t=i}^{j} d_t - x_g \sum_{t=i}^{j} g_t \left(= D_{ij} - x_g G_{ij} \right) \quad \text{(Equation 18)}$$

Thus, the required storage capacity is the magnitude of the difference between the total demand and the total generation during the bottleneck period when the difference is the largest.

The bottleneck period becomes shorter as the generation capacity increases. The relation is shown in Figure S2, where the horizontal axis represents time, and the light gray solid lines represent the normalized demand and PV generation profiles of the Tohoku region in 2018. Superimposed on that line is the transition of the bottleneck period, shown as the change in the period between the red lines. The bottleneck period is shown in relation to the generation capacity on the right side of the vertical axis. For $x_g = 1$ (the smallest generation capacity for 100% REPS), the bottleneck period is about nine months. As generation capacity increases, the bottleneck period becomes shorter, from about five months to a couple of days for $x_g \sim 1.5$.

The bottleneck period (sandwiched between the red lines) corresponds to the sunless and windless period or dark doldrums. Power generation is indeed smaller during this period. However, the sunless period does end, and the period varies depending on generation capacity.

Equation (Equation 18) can be seen as representing the energy balance in the bottleneck period. In that sense, the required storage capacity is equivalent to the shortage of power, that is, the difference between demand and generation when the difference is the largest, or the bottleneck amount.

Duality of linear function

As the variables (x, y) and coefficients/intercepts (a, b) of the linear function $y = -ax + b$ are dual, the following relations hold:

- A line in variable space corresponds to a point in coefficient space.
- The intersection of two lines in variable space forms a line segment between two points in coefficient space.
- The maximum value set in variable space represents (part of) the boundary of the convex hull in coefficient space.

Figure S3 illustrates the mentioned functions. In Figure S3A, 24 randomly generated straight lines are displayed in variable space. The maximum value sets of these lines are indicated by different colors, while their intersections are represented by dots within squares of different colors. The linear functions displayed in Figure S3A are represented as points in coefficient space in Figure S3B. Those corresponding to the straight lines (square points) in Figure S3A are represented by round points (line segments) of the same color.

Profile data

Hourly time series data for the demand and generation profiles (solar and wind) were collected from the website of the Organization for Cross-regional Coordination of Transmission Operators, JAPAN (OCCTO). The data cover a period of three years (fiscal year 2016–2018) and includes information from 10 regions in Japan.[36]

Criterion of economic feasibility for Japan's context

Based on discussions within the working group for generation cost estimation in the Ministry of Economy, Trade and Industry (METI) in Japan,[37] the generation cost of LNG power in 2030 is estimated to be between 10.7 and 14.3 JPY/kWh. Taking a conservative approach, this study adopted 10 JPY/kWh as the threshold for economic feasibility of renewable power systems in Japan. It is important to note that LCOHS represents the average cost for a 100% REPS, rather than the marginal cost.